Electrical Resistivity at Internal Erosion Locations in Levees

Stacey Tucker-Kulesza, *Associate Professor, Kansas State University, Manhattan, KS, USA; email: sekulesza@ksu.edu*
Cassandra Rutherford, *Assistant Professor, Iowa State University, Ames, IA, USA; email: cassier@iastate.edu*
Michelle Bernhardt-Barry, *Associate Professor, University of Arkansas, Fayetteville, AR, USA; email: mlbernha@uark.edu*

ABSTRACT: *Internal erosion through or beneath levees frequently occurs during flood events, resulting in sand boils. Determining the extent of damage from the seepage channels that caused the sand boils remains difficult, and many sand boils are simply monitored in subsequent floods. There is a need for a nondestructive methodology to map the voids caused by seepage channels so that needed repairs can be identified prior to the next flood. The objective of this study is to identify the electrical response of internal erosion pathways with electrical resistivity tomography (ERT). A case study using ERT on the Hager Slough Levee, which has experienced sand boils since the 1990s, is presented. Three ERT surveys were conducted along the levee in an area of apparent damage (i.e., crown settlement and sand boils) and where nearby boring logs were available. Laboratory resistivity tests provide support for the field ERT interpretations. The results indicate that ERT may be used to identify zones of damage within and beneath a levee. If used in practice, ERT has the potential to improve remediation of levees by identifying needed repairs.*

KEYWORDS: Electrical resistivity tomography, laboratory electrical resistivity, levees, sand boils, internal erosion

SITE LOCATION: **Geo-Database**

INTRODUCTION

A common problem during flood events is internal erosion, or piping, which often results in the formation of sand boils on the landside side of the levee. When the hydraulic gradient increases beneath the levee, the induced water seepage can carry soil particles from the toe of the levee or foundation, leading to piping, deterioration of the internal structure, and instability of the levee (Turnbull and Mansur 1959; Kolb 1975; Richards and Reddy 2007). Sand boils typically appear close to the toe; in some cases, however, visual detection of this seepage mechanism may be difficult because the sand boils can also occur hundreds of meters away from the levee (Schaefer et al. 2017). Temporary sand bag rings are used to control the water head on the sand boil and slow the water velocity, allowing water to continue to flow while minimizing the transport of material (USACE 2000). In many cases, minimizing seepage from one sand boil leads to the formation of additional boils in the surrounding area.

Most sand boils are left in place and are not repaired after a flood event. When the differential head of the flood subsides, the upward seepage in the flow channels and transported coarse-grained material slows and ultimately stops. The flow channels are then "filled" with coarse-grained material, creating preferred seepage paths which usually appear in the next flood. While the seepage can occur in subsequent events, the sand boils are monitored to ensure the transport of new material is minimized (USACE 2000). Large sand boils, or those which may impact the levee toe, are typically excavated and repaired. Relief wells and construction of landside seepage berms can also help decrease the occurrence of sand boils in extreme cases where a large number of boils repeatedly occur in an area (Mansur et al. 2000).

Although sand boils provide visual evidence that erosion has occurred, determining the extent of internal erosion damage within or beneath levees is difficult. Currently, there is no way to non-destructively evaluate or map the voids or the removal of fines within the levee or from its foundation soil, making it difficult to estimate the repairs needed on a section of levee.

The objective of this paper is to identify the electrical response of suspected internal erosion pathways with electrical resistivity tomography (ERT), a near-surface geophysical method. A case study using ERT on the Hager Slough Levee, which has experienced issues with seepage and sand boils since the 1990s, is presented. Soil boring logs taken in the area and laboratory electrical resistivity tests on samples collected from the sand boils provide support for the field electrical resistivity interpretations.

Hager Slough Levee

The Hager Slough Levee is located approximately 6.4 km northeast of Beardstown, Illinois, USA, on the south side of the Sangamon River (Figure 1). The city of Beardstown is in west-central Illinois along the Illinois and Sangamon Rivers. The Hager Slough Special Drainage District primarily manages the risk of flooding to farmland to the northeast of Beardstown, as well as a portion of the Toppers Hole State Conservation Area.
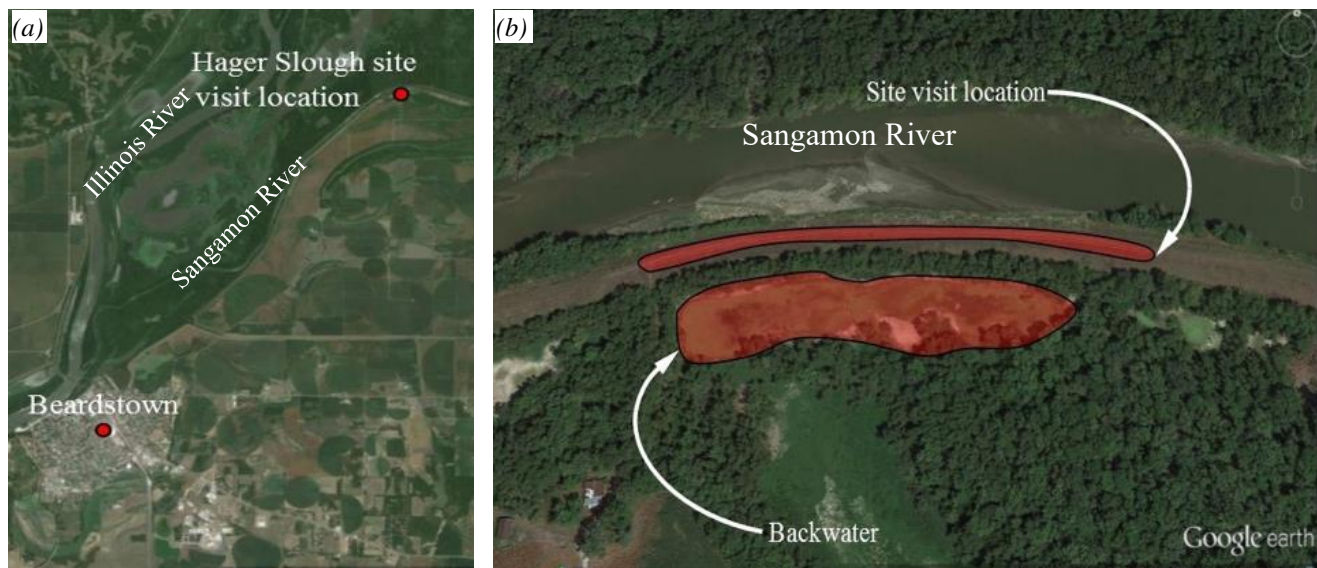

Figure 1. Experimental site: (a) location of Hager Slough Levee; (b) site visit location (Rutherford et al. 2016).

The Sangamon River is a principal tributary of the Illinois River flowing through central Illinois. The river is approximately 396 km long starting from Bloomington-Normal to Beardstown, Illinois. The Sangamon watershed is approximately 14,012 km^2. Historically, the Sangamon is known as "the River that Lincoln loved." Today, the Lincoln Heritage Canoe Trail follows the path along the Sangamon River that Abraham Lincoln traveled on in his flatboat to take supplies to New Orleans, Louisiana in 1831 before he was the 16th President of the United States. President Lincoln advocated for improving and clearing the river to accommodate large boats for commerce (Yeagle 2014).

The historic channel of the Sangamon River was originally 101 km long with a slope of 0.09 m/km. The river was channelized, and levees were built by local farmers to create drainage for the agricultural lands surrounding the river between 1905 and 1909. In 1949, the U.S. Army Corps of Engineers (USACE) diverted the lower 9.7 km of the river south through Muscooten Bay (Figure 2). In the 1980s, the river was straightened by the USACE to help with the silting of the Beardstown marina. Currently, the river channel is only 57.9 km long with an average channel slope of 0.19 m/km (Bishop et al. 2015). As a result of the straightening of the channel and diversion, the sediment load carried by the Sangamon River has been deposited in Muscooten Bay and its adjacent areas (Lee 1982). This caused silt and sandbars to form along the riverfront of Beardstown, causing issues with boating access in the marina (Jangea 2003) and the formation of log jams along the Sangamon River (Blanchette 2016). The USACE studied the problem by modeling the watershed and sediment transport, leading to a recommended sediment management plan (Bishop et al. 2015).

Figure 2. Sangamon River history: (a) Muscooten Bay pre-diversion (~1939); (b) Muscooten Bay post-diversion (~2011) (Bishop et al. 2015).

Geology

The Sangamon River and its tributaries were formed during the last interglacial episode. During the early Wisconsin Glacial Episode, the Sangamon River began to fill with sand and silt from the glacial outwash. Following the glacial retreat out of the Sangamon drainage basin, the river began a postglacial regime of a meandering stream with silt bars and natural levees (Miller 1973). The region is covered by generalized glacial deposits of alluvium, sand dunes, and gravel terraces formed from the Holocene and Wisconsin glaciations (Frankie et al. 1996).

Hager Slough Levee Concerns

The material that is now utilized as the Hager Slough Levee was initially stock-piled by dredging river delta material as a means to provide a straightened channel to mitigate the risk of damage from flood events and to provide drainage for the upstream agricultural fields. Holes were left in the spoil piles to allow the Sangamon to connect to its floodplain. In the 1970s, downstream farmers wanted protection from flood events and filled in the gaps in the spoil piles with sand and clay. The downstream farmers also built a clay tieback levee at the confluence of Indian Creek and the Sangamon River, creating the Hager Slough Special Drainage District. The upstream tieback was a clay levee built by local interests in the early 1900s and is part of the Clear Lake Drainage District. Together the two districts share responsibility for providing flood risk management to approximately 5,700 Ha of farmland. The districts meet at the intersection of the Sangamon channel spoil pile and Black Slough. Over the years, the river-dredged materials were capped with a clay layer. A simplified typical cross-section of the levee is shown in Figure 3. The crest was approximately 3.8 m wide and the levee height approximately 4.57 m at the surveyed levee section in this study.
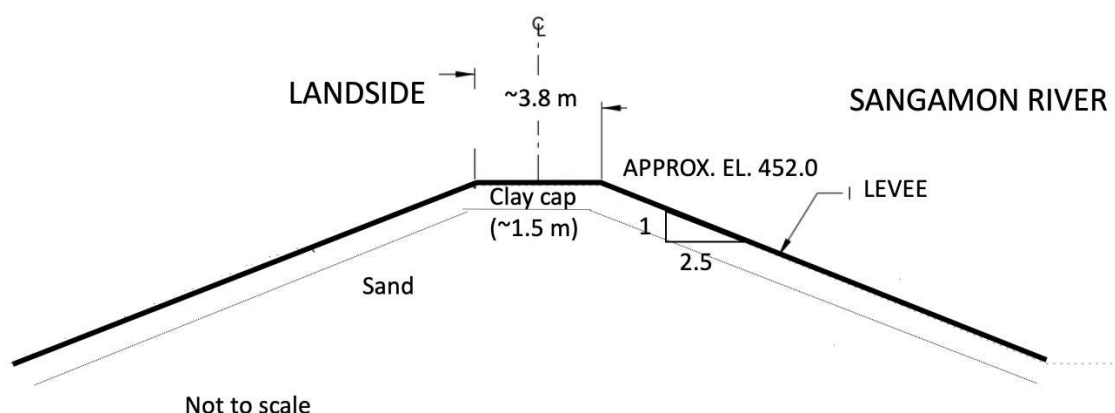
APPROX. EL. 137.8m

Figure 3. Hager Slough Levee pre-repair simplified cross-section.

The levee district officials and the USACE engineers have observed a large number of sand boils at the Hager Slough Levee toe during flood events over the last thirty years (Bishop et al. 2015). In December of 2015, unusual winter storms related to a strong El Niño weather pattern in the Midwest sent large volumes of water into rivers and drainage areas, causing historic flooding in Illinois. As part of the flood protection systems investigation in Illinois, a team from the Geotechnical Extreme Events Reconnaissance (GEER) Association was mobilized to investigate the impacts of record and near-record flood crests and the performance of levee systems (Rutherford et al. 2016). The Hager Slough Levee was inspected and damage in multiple locations was documented on January 8, 2016. There were upwards of 15 active (carrying material) sand boils and many inactive (clear flowing water) sand boils from previous flood events which were documented during the reconnaissance. New (active at the time) sand boils generally formed adjacent to the existing boils. There were upwards of 41 sand bag rings placed by the levee district in coordination with the USACE in the 0.4 km levee stretch covered during the site visit. Many of the sand bag rings contained numerous sand boils and seeps. The sand bag rings were typically 2.43 – 3.00 m in diameter and 0.610 – 1.22 m in height (Figure 4).
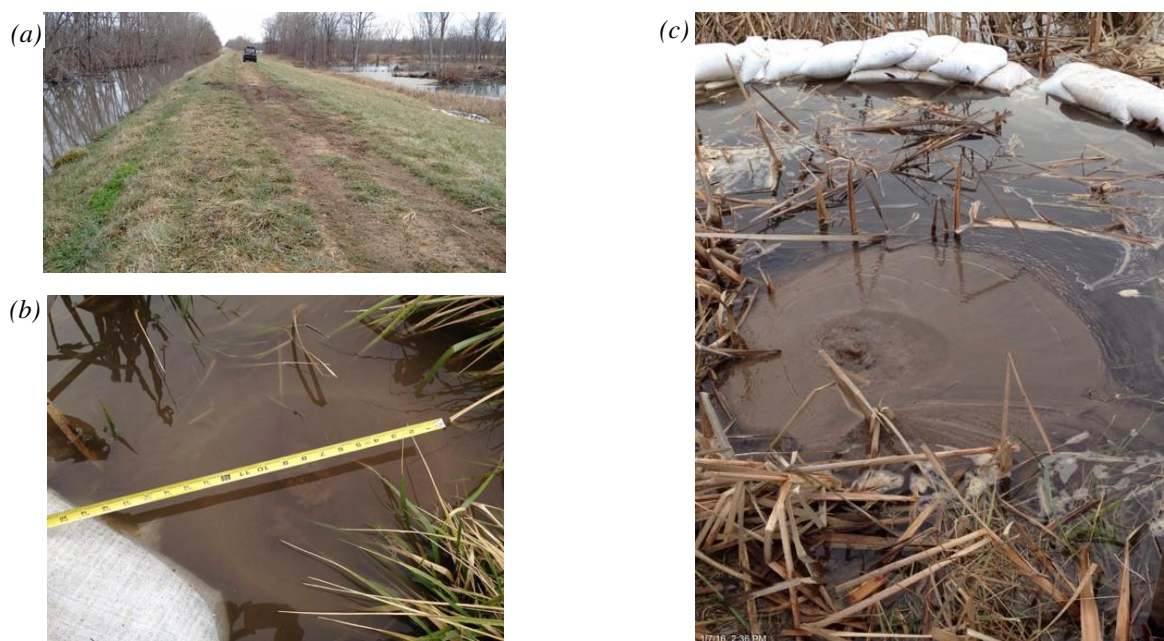

Figure 4. Observed damage during December 2015 flood event: (a) crown of levee, (b) 0.33 m diameter active sand boil, (c) active sand boil (Rutherford et al. 2016).

Settlement of the levee crown occurred in several locations during the 2015 flooding which required repair (repair images not available). Subsidence of the levee crown in these locations was observed to be adjacent to sand bag rings (Figure 5), suggesting that the subsidence was due to material loss. The objective of the geophysical investigation described in this study was to evaluate if ERT can be used as an imaging technique to detect zones of material loss within the levee. Such a system would enable improvement of remediation methodologies following flood events where sand boils occur. ERT may also be used to evaluate if a levee is damaged internally despite the lack of external physical evidence (e.g., sand boils). Following this introduction are a brief background on ERT and the research methodology. The ability of ERT to identify material removal has been investigated by performing a series of ERT surveys and supported with soil borings and a laboratory electrical resistivity measurement of the material in the sand boils. A discussion of the field and laboratory results is presented, including limitations of this case history, followed by conclusions and recommendations.

Figure 5. December 2015 flood reconaissance: (a) settlement of crown with active sand boil at toe of levee, (b) active sand boil with sand bag ring (Rutherford et al. 2016).

ELECTRICAL RESISTIVITY TOMOGRAPHY

Electrical resistivity is an intrinsic material property that indicates the material's ability to oppose the flow of electric current. The electrical resistivity of soil is a function of water content, ionic concentration, soil density, and grain size distribution (Fukue et al. 1999). Because it is an intrinsic soil property, electrical resistivity is becoming increasingly popular for geotechnical investigations (Mofarraj Kouchaki et al. 2019; Karim and Tucker-Kulesza 2018; Kermani et al. 2018; Kimbra and Hossain 2016; Sirieix et al. 2015; Abdeltawab 2013). Electrical resistivity tomography (ERT) measures the spatial distribution of bulk electrical resistivity in the subsurface using a series of electrodes arranged in a straight line at the surface. Four electrodes are commonly used for apparent resistivity measurement: two induce current flow (I) into the subsurface and two measure the resulting voltage potential difference (V). The term apparent resistivity, ρ_a, indicates the resistivity of an ideal homogeneous subsurface. The apparent resistivity is

$$\rho_a = \left(\frac{2\pi V_{\mathrm{PQ}}}{I}\right)\left[\frac{1}{r_{\mathrm{AP}}} - \frac{1}{r_{\mathrm{AQ}}} - \frac{1}{r_{\mathrm{BP}}} + \frac{1}{r_{\mathrm{BQ}}}\right]^{-1} \qquad (1)$$

where V_{PQ} is the measured voltage difference between electrodes P and Q, I is the induced current, and r is the distance between the current electrodes (A and B) and the voltage electrodes (P and Q). Multiple pairs of voltage electrodes with different relative separations are used for each current injection in ERT surveys to sample different volumes and assess the heterogeneities of the subsurface. The survey depth of penetration and resolution are controlled by the distance between the electrodes and the sequence of the measurements, or the array type. There are three commonly used ERT arrays: dipole-dipole, Wenner, and Schlumberger; however, modern data acquisition systems allow for combinations of standard arrays and non-standard electrode sequences. Both standard and non-standard arrays have different trade-offs in terms of the depth of penetration of the signal, signal-to-noise ratio, vertical and lateral resolution, and survey time. The dipole-dipole array was used for all surveys in this study because it yielded a compromise between vertical and lateral resolution and had minimal coupling effects between the electrode pairs (Binley and Kemna 2005). The distance between the two current electrodes and two voltage electrodes was the same while the distance between the two pairs increased by a factor n (Figure 6). The data quality was limited near the surface; however, the near-surface volume (i.e., $0.3 - 0.7$ m depending on the electrode spacing) was not of interest in this study.
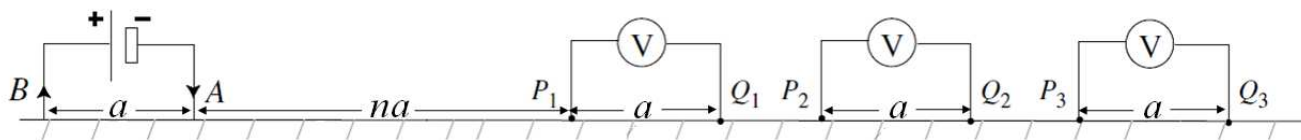

Figure 6. Dipole-dipole array.

Over 2,000 apparent resistivity measurements were obtained for each survey in this study. These data were transformed through an iterative process of forward modeling and inversion to obtain the true resistivity of the subsurface. The Advanced Geosciences, Inc. (AGI) *EarthImager 2D* commercial software was used in this study to invert all data (AGI 2009) with an Occam style smooth model inversion (Constable et al. 1987). The objective of a smooth model inversion is to obtain the minimally rough, or maximally smooth, model that best fits the data. Smooth model inversions allow resistivity values to undulate smoothly through the model domain, which yields more stable solutions and minimizes mathematical artefacts as compared to other inversion methods (Loke et al. 2003). In *EarthImager 2D*, the user estimates the root mean squared error (RMS) between the field measurements and model data. The RMS and L2-norm (i.e., the sum of the weighted, squared differences between the field measurements and model data) are used as data misfit criteria in the inversion. The objective of the inversion process is to meet the data misfit criteria in as few iterations as possible, where up to ten iterations are generally acceptable. An RMS error less than 10% is an acceptable fit for most geotechnical applications (Tucker et al. 2015). All inversions in this study had RMS less than 10%, L2-norm less than unity, and converged within eight iterations.

METHODOLOGY

Field Testing

Three ERT surveys were conducted at the Hager Slough Levee. The survey locations were chosen in an area where damage was apparent (i.e., crown settling and sand bags around previous sand boils) and borehole data were available for ground truthing. The crown settlement was estimated between 0.12-0.14 m based on survey data. The three survey lines are shown in Figure 7. Two overlapping survey lines were conducted along the levee crown and one was conducted parallel to a 5 m diameter sand bag ring shown in Figure 7 at the landside toe. Stainless steel stakes were used as contacts between the 56 electrodes on the cables and the subsurface. The electrodes were spaced at 2 m, 1 m, and 0.5 m in Lines 1, 2, and 3 respectively. Lines 1 and 2 were aligned so that the visible 2 m wide depression from the crown settling was approximately in the middle of the surveys (marked with a star in Figure 7). The larger electrode spacing in Line 1 allowed for deeper measurements while the 1 m spacing in Line 2 resulted in more detailed measurements near the surface. The relative elevation at each electrode was collected with a total station, although the elevation change cannot be seen in the crown surveys (Lines 1 and 2) due to the length of the survey relative to the elevation changes. The closest borehole was approximately 73 m west of the crown settlement, where samples were collected by the USACE through the levee to 9.45 m in 2013.
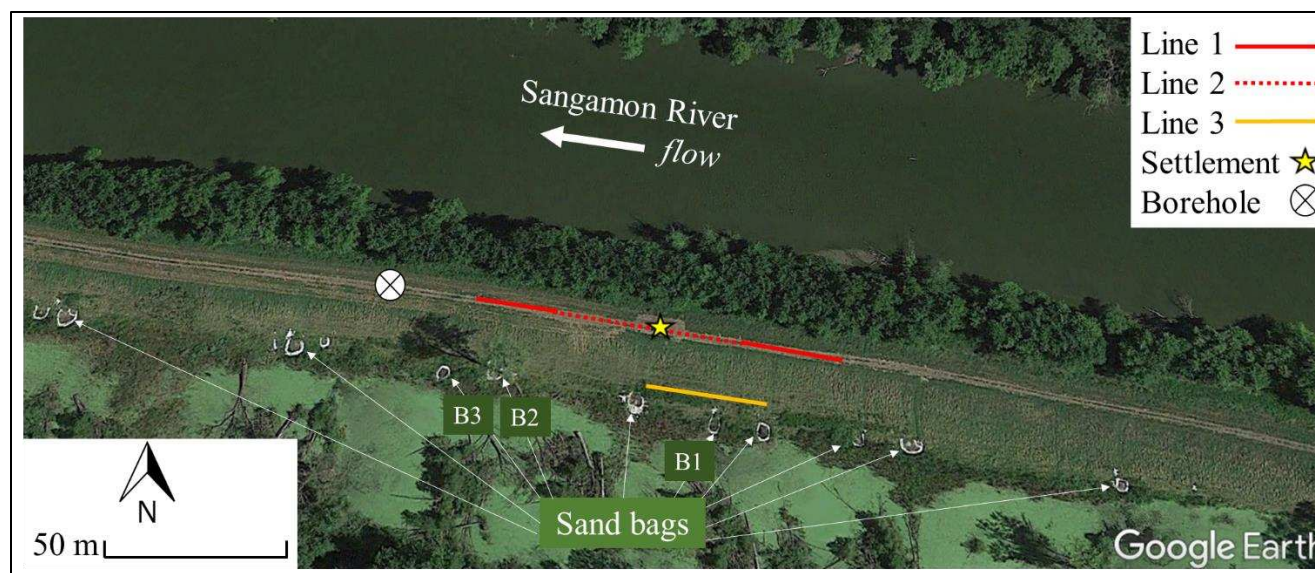
Figure 7: Survey locations; white rings are remaining sand bags from January 2015 flooding (Google Earth 2015). B1, B2, and B3 indicate where grab samples were collected for the laboratory analysis.

Although the ERT surveys conducted in this study are shown as 2D results, the flow of electric current in the subsurface is 3D; therefore, ERT images are commonly referred to as 2.5D images. Project sites with variation in bulk electrical resistivity, such as a highly conductive (low resistivity) body of water, or where geometry perpendicular or directly beneath the survey line changes such that the current flow may encounter a soil/air interface, must consider 3D effects. Snapp et al. (2017) conducted ERT surveys on mechanically stabilized earth wall backfill during construction and showed that the effects of the wall face (and infinitely resistive air on the front side) do not influence the measured resistivity if the survey is performed at least one electrode spacing from the discontinuity in electrical resistivity. The crown of the Hager Slough Levee was 3.8 m wide and the levee had 1V:2.5H slopes. The maximum depth of each apparent resistivity measurement was taken as the median depth, z_{med}, which is the depth at which half of the electrical current flow is above and half of the electrical current is below. Most inversion software, including *EarthImager 2D* (AGI 2009), use the median depth, defined by Edwards (1977)

$$n(n+1)(n+2)\{[n^2+u]^{-1/2} - 2[(n+1)^2+u]^{-1/2} + [(n+2)^2+u]^{-1/2}\} = 1 \qquad (2)$$

where $u = 4(z_{med}/a)^2$

in which n and a are defined in Figure 6. The electrode spacing in Line 1 was 2 m, centered on the crown. The uppermost measurement of Line 1 was 1.4 m into the levee, which occurred 3.5 m laterally from the slope/air interface on both sides of the levee. The electrode spacing in Line 2 was 1 m, with an uppermost measurement at 0.42 m. The uppermost Line 2 measurement occurred 1.05 m from the levee slope/air interface. Furthermore, this levee/slope interface would likely concentrate the flow of electric current into the core of the levee. Note that as the measurements were collected deeper into the levee, the distance from the slope/air interface also increased. As the data are only interpreted by a 2D inversion algorithm, the levee slope/air interface may cause an artificial 3D increase in the calculated subsurface resistivity (in this case, resistivity of the levee). However, note that these 3D effects would be the most critical in the near surface regions closest to the crown where measurements were in the range of 20-40 Ωm (i.e., the expected range for clayey soils which were known to be present as shown in Figure 3). Therefore, current flow 3D effects encountered in infrastructure problems where there is a soil/air heterogeneity perpendicular to the survey line were negligible in this study.

Laboratory Testing

Laboratory-based electrical resistivity testing was conducted on bulk samples retrieved from the sand boils located along the landside toe of the levee. Samples were collected from three sand boils. An additional sample of the material contained within the sand bags was taken to help distinguish between the transported material and what could have been spilled material from

the sand bags. A Nilsson Resistance Meter Model 400 attached to a M.C. Miller Large Soil Box (270 mL volume) was used to obtain the electrical resistivity for the laboratory specimens (Figure 8). The soil box uses a 4-electrode array in which electrical current is passed through the soil using two external (current) electrodes and the voltage potential is measured across two internal (voltage) electrodes inserted into the soil (Herman 2001). The electrical resistivity of the specimen in the soil box can then be calculated using

$$\rho = \frac{RA}{l} \tag{3}$$

where R is the electrical resistance measured by the voltage electrodes in Ohms (Ω), A is the cross-sectional area of the specimen in cm^2, and l is the distance between the voltage electrodes in cm (ASTM G57 – 06, 2012). The cross section to length ratio (A/l) of the soil box used was 1 cm, meaning that the measured electrical resistance (Ω) has the same numerical value as the electrical resistivity (Ωcm).

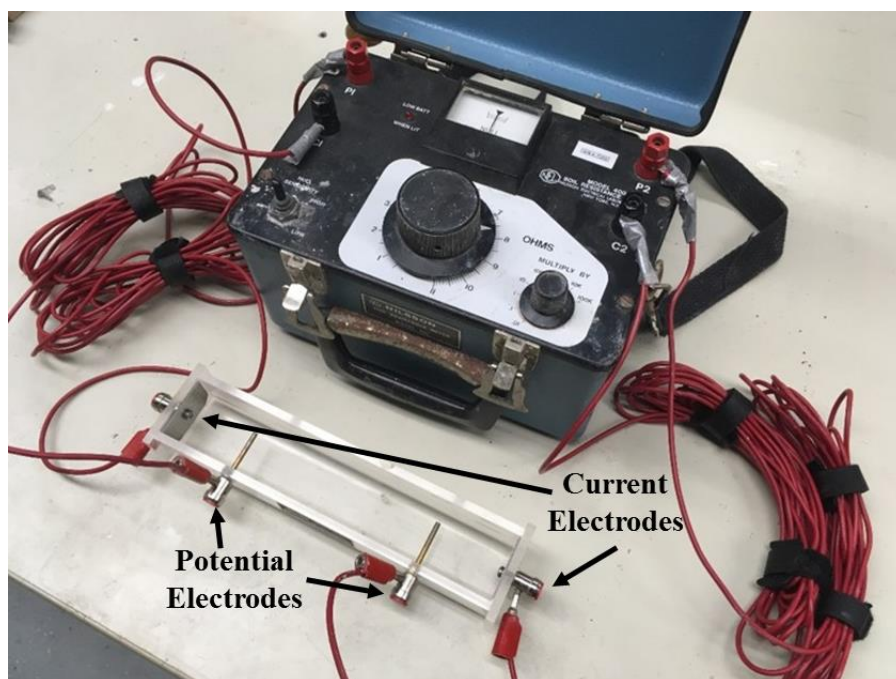*Figure 8. Laboratory resistivity setup.*

Oven-dried specimens were weighed and mixed with deionized water to high degrees of saturation (> 60%) to determine the minimum electrical resistivity (AASHTO T 288; Mofarraj Kouchaki et al. 2019). Deionized water was used so that no additional ions were introduced in the soil or pore fluid. Additionally, Mofarraj Kouchaki et al. (2019) showed that water mineralization does not largely affect the electrical resistivity for higher degrees of saturations like those used in this study. The soil was placed in three equal layers to ensure a uniform specimen and the total weight of the soil box was recorded for bulk density calculations. The electrical resistivity and temperature of the specimens were measured and recorded. The water content of the specimens was also verified at the end of each test. All results were corrected for temperature differences between the laboratory and field conditions. More details of the setup and procedures can be found in Mofarraj Kouchaki et al. (2019).

RESULTS AND DISCUSSION

Field Results

Three ERT surveys were conducted at the Hager Slough Levee: two survey lines on the crown of the levee and one survey line at the landside toe. Figure 9 shows Line 1 (top, a) and Line 2 (bottom, b), which were conducted along the levee crown as shown in Figure 7. The depression in the crown is again marked with a star on each inverted image and the survey alignment with a ring of sand bags at the toe of the levee is also shown. The horizontal distance along the crown is depicted on the top

of each survey and the elevation above sea level is on the side of each survey, both in m. Line 1 was 110 m long with a maximum survey depth of 27 m (El. 110.8 m). The approximate location of the native soil based on the height of the levee is shown with a dashed line in Figure 9. Borehole data were available approximately 73 m west of the first electrode in Line 1. Because of the depth of investigation and scale of Figure 9(a), the borehole data are also shown to the right of Figure 9(b) so that the stratigraphic units could be aligned with the image and compared with geophysical interpretations.

The soil stratigraphy based on the borehole consisted of: 1.4 m of sandy lean clay (CL), 4.2 m of poorly graded fine sand (SP), 0.3 m of fat clay (CH), 1.5 m of sandy lean clay (CL), and 1.3 m of poorly graded sand with clay (SP-SC) until the boring was terminated. The water level was noted at El. 132.2 m, near the interface of the fat and lean clays as shown in Figure 9. The river level was measured at approximately the same elevation. The color-coded electrical resistivity scale and approximate Unified Soil Classification System (USCS) classifications, based on the borehole data and general soil type classifications of ERT data, are shown beneath the inversions (ASTM D2487 2011; Everett 2013; Sharma 1997). The observed electrical resistivity from the ERT profile in Figure 9(a) is a low resistivity layer of 25-40 Ωm in the top 2 m over a layer of higher resistivity (~150 – 300 Ωm). The higher resistivity layer thickness varies from approximately El 135.8 m to El 129.8 m along the profile in Figure 9(a). The layer of higher resistivity aligns well with the SP layer identified in the borehole from approximately 60 m to 110 m along the profile. From 0 m to 60 m, the high resistivity layer penetrates to El 129.8 m, where the deepest point is at the 48 m marker on Figure 9(a). Note that this point was located two electrode spacings from the depression in the crown. The bulk electrical resistivity beneath the high resistivity zone was between 60 and 80 Ωm in the rest of the inversion, except beneath the 60 to 74 m markers where a zone of lower resistivity (47 –50 Ωm) was noted. No resistivity measurements are shown outside the trapezoidal ERT inversions because ERT measurements are only marginally sensitive in these regions.
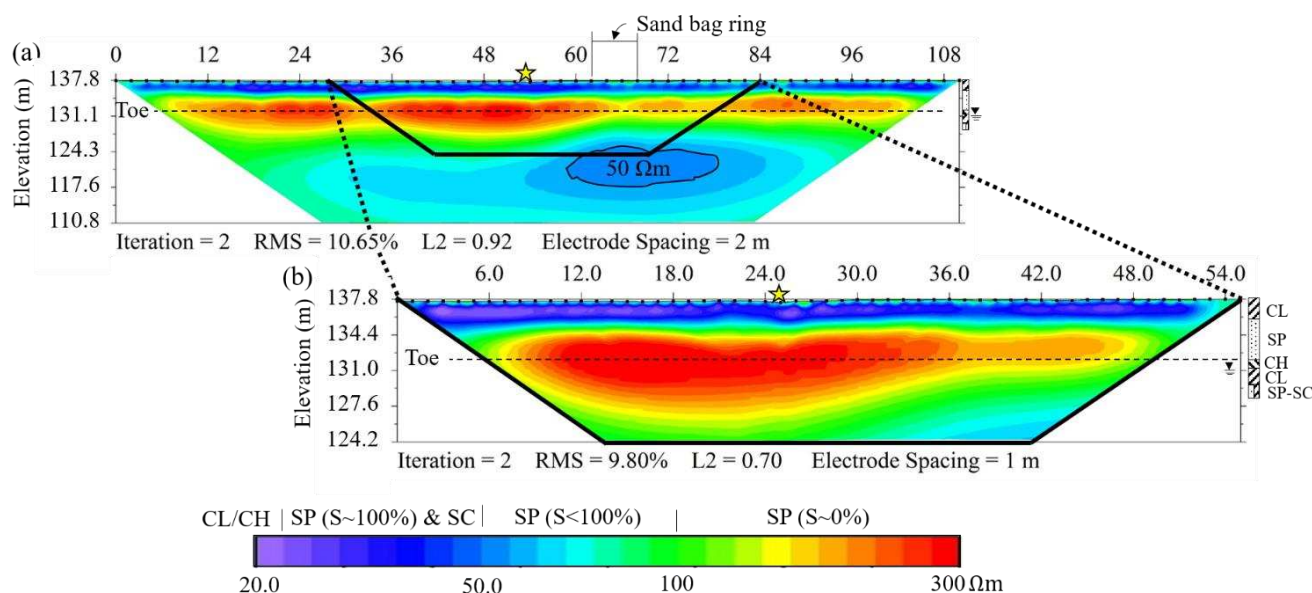

Figure 9. Crown surveys: (a) Line 1 with 2 m electrode spacing; (b) Line 2 with 1 m electrode spacing.

Line 2 (Figure 9(b)) was conducted at half the electrode spacing of Line 1. The outermost 14 electrodes on both sides of the central point in Line 1 were removed and installed between the remaining 28 electrodes. The alignment of Figure 9(b) within Figure 9(a) is shown with a black trapezoid on Figure 9(a). The larger electrode spacing in Figure 9(a) increased the penetration depth of the survey; however, near surface resolution was lost as a trade-off. Therefore, the lower resistivity band is more apparent in Figure 9(b) than in Figure 9(a), varying from 20 – 25 Ωm. A band of higher resistivity (200 – 300 Ωm) is again noted beneath the low resistivity layer along the surface. In Figure 9(b), the depth of this higher resistivity layer varies from El. 134.4 m to El. 129.4 m. There is a bowl shape of the higher resistivity layer in Figure 9(b), with the maximum curvature approximately 3 electrode spacings from the depression in the crown of the levee. The small pocket of lower resistivity (60 Ωm in Figure 9(b)) is observed in the lower right side of the inversion, though the depth of penetration of this signal did not allow the entire region to be captured. Although the borehole data were approximately 99 m from this survey,

the data are shown along with the measured groundwater table in Figure 9(b). The soil stratigraphy aligns well with the geophysical measurements in the upper 5 m of the levee from 36 to 48 m along the profile.

There are relatively thin layers between the higher and lower resistivity zone discussed in both surveys. These should not be interpreted as additional soil layers, but rather as smoothing effects. ERT surveys collect bulk measurements with depth, and a trade-off of the mathematically stable Occam style smooth inversion smears at sharp boundaries, preventing the defining of sharp layer interfaces with depth. This smearing effect is especially noted in Figure 9(a) where the resistivity in the upper 2 m appears to be higher and less uniform than in Figure 9(b), where higher resolution data were collected near the surface. The smearing effect is still noted between the two layers in Figure 9(b), though it is minimized.

Line 3 (shown in Figure 10) was conducted approximately 3 m above the levee toe on the land side of the levee. The survey in Figure 10 was approximately 5.1 m from the center of the sand bag ring labeled in Figure 9(a). No nearby borehole data were available; the depth to the groundwater table based on the boring from the crown of the levee, however, is shown on the right side of the inversion. The uppermost layer to El. 133.9 m was low resistivity, from 15 – 20 Ωm, similar to the upper layer in Figure 9(b). There is a layer from El. 133.7 m to El. 132.7 m that has resistivity values between 30 and 75 Ωm. The bottom layer is less than 30 Ωm and likely corresponds to the approximate groundwater table as shown. Note that relative resistivity color scheme was changed in Figure 10 to improve visualization of the inversion.
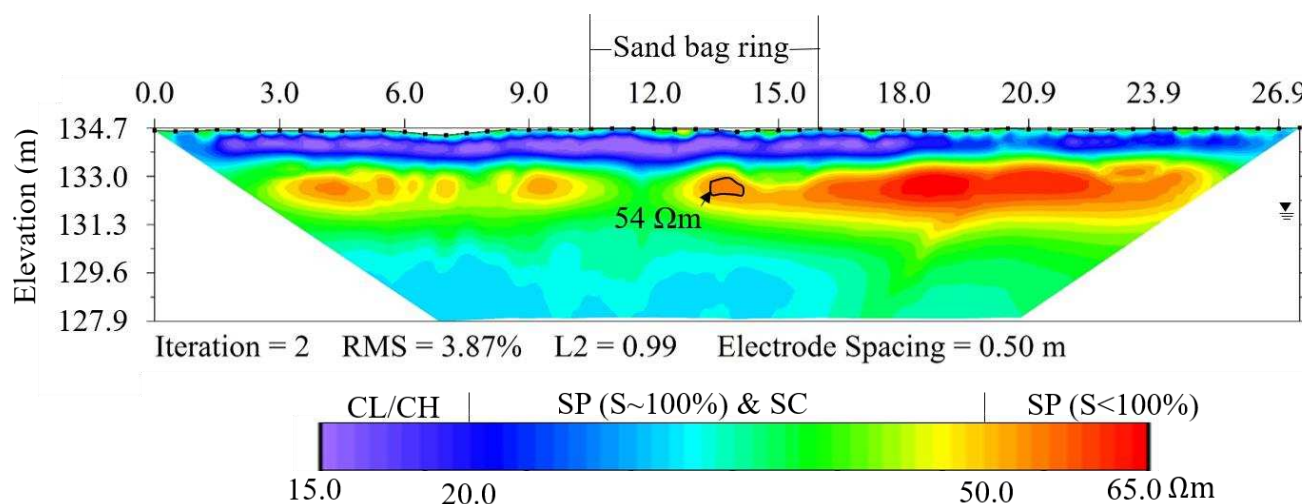

Figure 10. Line 3, survey near the landside toe that was 5.1 m uphill of sand bag ring.

Laboratory Results

Table 1 provides the measured and corrected minimum electrical resistivity values and corresponding test conditions for the sand boil specimens. There is a clear distinction in resistivity for the sand bag material collected as compared to the other soils collected within the boils. Sample B1 was sampled from within the sand bag ring labeled on Figures 7, 10, and 11. Samples B2 and B3 were collected from other sand boils as labeled on Figure 7. Note that Samples B2 and B3 only aligned with Line 1 and were in the regions where little to no ERT data were collected along the edges of the survey. Therefore, sample B1 was the main focus of the laboratory study.

Table 1. Minimum resistivity results for sand boil specimens as determined in the laboratory.

Boil No.	Test Resistivity (Ωm)	Test Temperature (°C)	Corrected Resistivity @ 15.5 °C (Ωm)	Corrected Resistivity @ 18°C (Ωm)	Bulk Density (kg/m³)	Water Content (%)	USCS Classification
B1	22.8	22.3	26.1	25.3	2044.8	18.2	SM
Sand Bag	138.0	22.8	163.2	154.6	1864.3	11.0	SP
B2	70.2	23.4	84.1	79.7	1959.0	15.1	SP-SM
B3-red	78.5	22.6	92.4	87.5	1872.7	19.5	SP

Because of the location of sample B1 within the ERT profiles and the higher fines content, a further investigation of the possible ranges of electrical resistivity values was conducted. Unfortunately, no information was available regarding the in situ density of the sand boil material or of the samples characterized by the USACE. Therefore, by running the laboratory samples at a range of densities at the same water content, a range of possible field electrical resistivity values could be interpreted. It is noted that although only a few of the trials are detailed here for brevity, specimen B1 was tested at a large range of water contents and densities to establish an "envelope" of values possible in the field. Table 2 shows the electrical resistivity values for B1 compacted at different densities at a water content of 10.3%. This water content was lower than the saturated water content used to determine the minimum resistivity in Table 1 and it represented the water content which led to the largest possible range of densities that were likely to occur in the field. The field results also indicated that the zone of interest was likely not in a saturated state. The values in Table 2 correspond to the upper and lower bounds of bulk density expected in the field. Although ASTM G57 corrects the resistivity to 15.5°C, an additional corrected value to 18°C was calculated as these temperatures were more representative of the in situ conditions during the summertime testing.

Table 2. Resistivity of sample B1 for varying densities.

Boil No. – Trial No.	Test Resistivity (Ωm)	Test Temperature (°C)	Corrected Resistivity @ 15.5 °C (Ωm)	Corrected Resistivity @ 18°C (Ωm)	Bulk Density (kg/m^3)	Water Content (%)
B1-2	57.5	24.0	69.7	66.1	1532.8	10.3
B1-3	37.5	24.1	45.6	43.2	1746.9	10.3

Sample B1 classified as a silty sand (SM) based on the USCS classification (ASTM D2487 2011); however, there was no SM identified in the soil borings by the USACE. Determination of the percent fines by washing (ASTM D1140 2017), particle size analysis of the coarse fraction by sieve (ASTM D6913 2017), and particle size analysis of the fine-grained fraction by hydrometer (ASTM D7928 2017) were conducted to determine whether this soil was a mixture of the sand fill and clay levee material shown in the boring log or a foundation soil located deeper than what was captured in the USACE boring. Figure 11 shows the particle size distribution curve for sample B1. The soil contained approximately 68% sand particles and 32% fine-grained particles passing the No. 200 sieve, of which approximately 3.5% were clay sized particles (i.e., < 0.002 mm). This soil was comprised of approximately 28% silt sized particles. The large fraction of silt size particles and the fact that a silty soil was not identified on the boring log suggested that the soil came from locations deeper than what was captured by the available boring. The low percentage clay fraction obtained also indicated that this soil was a different soil altogether and was not a mixture of the sand and clay soils resulting in a SM classification. The liquid limit and plastic limit of sample B1 were determined to both be 19 (following ASTM D4218 2017), resulting in a non-plastic designation for the fines.
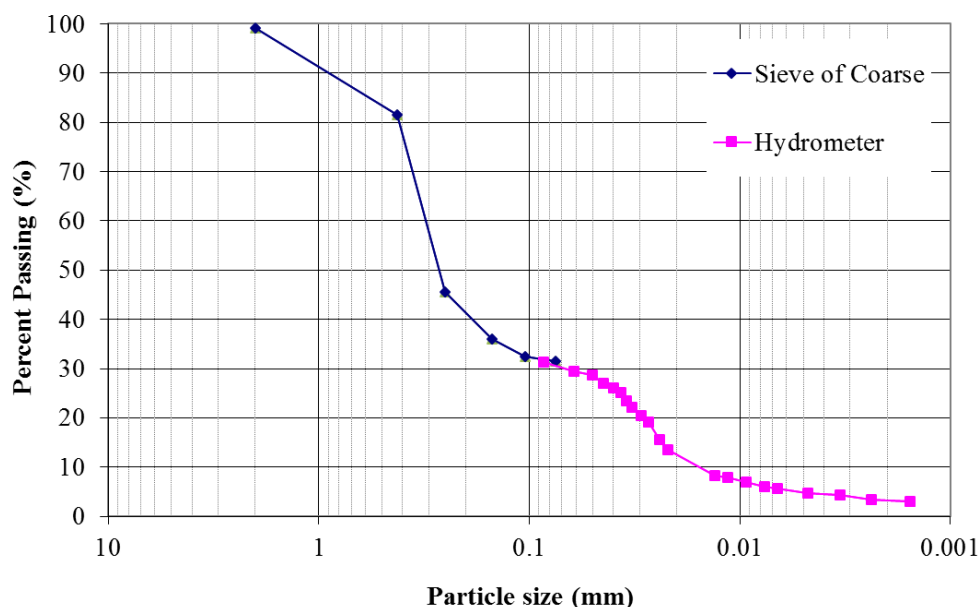

Figure 11. Particle size distribution for sample B1 retrieved from Sand Boil 1.

Discussion

The objective of this study was to identify the electrical response of suspected seepage channels nondestructively using electrical resistivity measurements. The Hager Slough Levee was selected because of the extensive numbers of sand boils that were observed in the 2015 flooding (Rutherford et al. 2016), the site availability which allowed access to the sand boil materials for laboratory testing, and the borehole data collected by the USACE in preparation for levee repairs. Three ERT surveys were conducted: two aligned with apparent damage to the crown and one with a sand bag ring that was 11.5 m east of the crown settlement. Figure 12 shows Line 1, the 2 m spacing survey conducted at the crown, and Line 3, conducted near the landside toe of the levee. The dashed lines show the alignment between the two surveys. Note that the color scale between the two surveys is different to improve visualization.
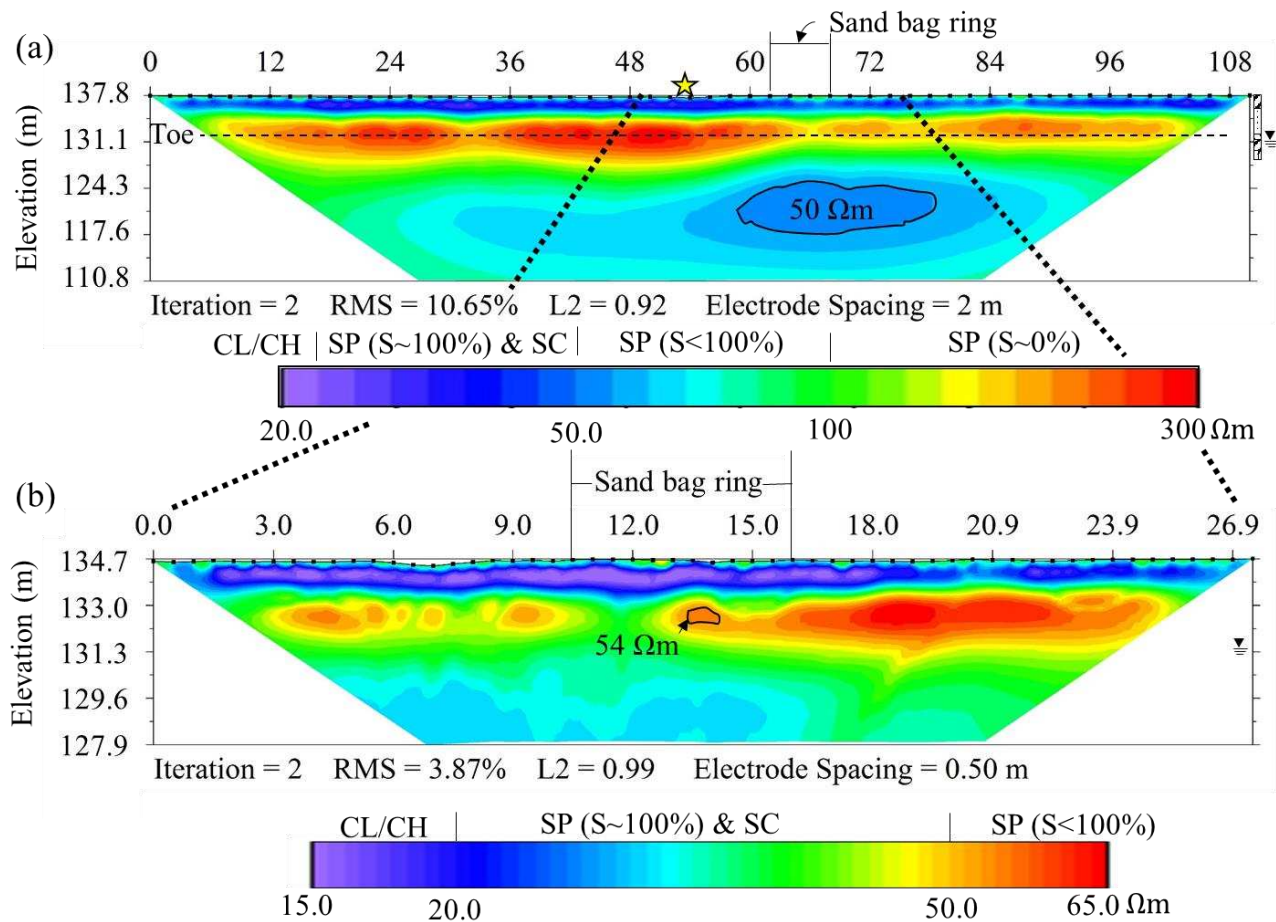

Figure 12. Alignment between Line 1 at the levee crown and Line 3 near the levee toe.

The uppermost clay layer is apparent in both surveys, although it is clearer in Figure 12(b) where the electrode spacing is smaller and the near surface resolution greater. The electrical resistivity of clayey soils (CL/CH) is typically between 1 - 20 Ωm (Everett, 2013). As shown in Figure 3, the levee was constructed of sand with a clay cap. Therefore, a zone of higher resistivity was anticipated beneath the clay layer. The sandy material (electrical resistivity between 150 - 300 Ωm) was noted in Line 1 and aligned with the nearby borehole data; however, it was not present in Line 3. Note from Figure 12 that the approximate interface between the levee and foundation materials was at El. 133.5 m, therefore minimal sand was expected at Line 3. Line 3 allowed for a more focused interpretation of the anomalous zone of 50 Ωm that aligned with the sand bag ring in Line 1. Zones of relatively higher resistivity between 50 - 65 Ωm were identified in Line 3, including one discrete zone that was centered along the alignment of the ring of sand bags at the toe of the levee. Figure 12(a) also includes a zone of lower resistivity (approximately 50 Ωm) that aligns with the ring of sand bags and extends to the edge of Line 3. The

remaining material beneath the toe of levee in Figure 12(a) is between 70 - 100 Ωm and likely a partially saturated coarse-grained material based on the location of the groundwater table from the USACE data.

Laboratory electrical resistivity measurements were used to determine if the material found in the sand boils could be related back to the ERT surveys to determine the zones or locations of the seepage, and thus the transported material. Laboratory electrical resistivity measurements are dependent on the density of the specimen in the apparatus, so a range of densities were tested to determine the range of electrical resistivity that could be measured in the field. Note that the laboratory measured electrical resistivity does not fluctuate significantly when samples are fully saturated for soils at the same density and temperature. The laboratory resistivity of the material collected from within the sand bag ring was 43 – 66 Ωm. This range of electrical resistivity encapsulated the measured field electrical resistivity in the unknown region in Line 1 and Line 3. The discrepancy between the field and laboratory measurements may be due to variable water content, density, or temperature. Note that the electrical resistivity of the sand bag material was also tested in the laboratory. The sand used to fill sand bags and the sand used to construct the levee were the same according to the USACE. The minimum resistivity for the sand bag material shown in Table 1 was 154.6 Ωm, which corresponded to the measured resistivity of the levee from the crown and was well above the electrical resistivity of the material within the sand bag ring.

By combining the laboratory and field electrical resistivity with the approximate areas of seepage based on the sand bags at the site, it was likely that these zones of 50-60 Ωm in Line 1 and Line 3 represent the zones in which the seepage and material transport occurred, carrying these soils under the levee and to the sand boils at the levee toe. In Line 1, the seepage channel appears to spread between the 58 and 76 m markers, but again resolution is lost with depth. Line 3 aligns with the Line 1 damage, showing higher resistivity from approximately 13 to 26 m. More discrete zones where material may have been moved under the levee and to the sand boils are seen in Line 3. The regions of the seepage channels in Line 3 are much closer to the surface than in Line 1 because they are closer to the sand boil "exit" and the material is working its way to the surface. The change in electrical resistivity within these potential seepage channels relative to the undisturbed soils may be due to a combination of many factors. The seepage force displacing the particles will likely alter the soil porosity as particles are displaced. The pore fluids within this seepage channel may be different than the native pore fluid, changing the ionic composition of the pore water. The seepage may have caused the removal of finer particles, or the removal of surface conductance of the fine particles. Unfortunately, the cause of the change in electrical resistivity relative to the native soil could not be identified because no samples could be collected from the identified anomalies beneath the levee at the time of the ERT survey. Therefore, the primary limitation of this study was that these interpretations of the seepage channels were based on laboratory and field resistivity measurements alone. Subsequent ground truthing where the surveys were conducted is the only way to definitively support this interpretation.

ERT can also be used to identify the original ground surface elevation based on the known electrical response of geo-materials, and therefore also the height of the levee if there is strong contrast between the foundation soils and levee materials. In this study, the variable "height" of the levee as interpreted from the high electrical resistivity typical of sand in Line 1 and 2 may be from uneven terrain. The levee was originally constructed using dredged sand to a predetermined flood stage height; this extra sand may have been required to maintain a constant freeboard (height). The top of the sand layer is fairly consistent across Lines 1 and 2, except near the settlement in the crown noted at the surface. As expected, the nearby material was also displaced and shifted down near this region. Note that the seepage channels that caused sand boils B2 and B3 may have further contributed to the variable displacement of the sand core in this region.

Following the field investigation and surveys presented in this study, the USACE completed rehabilitation work to mitigate the seepage issues on the Hager Slough Levee. A 960.4 m sand seepage berm was constructed on the landside toe of the levee and a turtle mitigation berm was constructed on the riverside toe of the levee in July 2017. The berms were constructed using approximately 60,000 m^3 of sand dredged from the adjacent Sangamon River channel.

CONCLUSION

A case study on the Hager Slough Levee in Illinois, USA was presented to illustrate the potential use of ERT to identify locations and the extent of erosion pathways within the levee. ERT surveys were directly aligned with areas where internal erosion was observed by sand boils and localized settlement on the levee. ERT image interpretations were supported with soil borings and laboratory resistivity measurements. An advantage of ERT is the ability to identify heterogeneous soil inclusions within an assumed homogeneous soil. From the ERT surveys, a localized zone of low resistivity was identified, which had a lower resistivity than the surrounding soil. This zone appeared on several of the ERT survey lines, likely indicating a zone of disturbance and internal erosion. This interpretation was further explored through laboratory testing on

the retrieved sand boil samples. Although no field proof of the internal erosion was collected through sampling or excavation pits at the time of the study, interesting evidence was collected which suggests that the soils retrieved from the sand boils were representative of the material identified in the ERT surveys.

Laboratory tests on the sand boil sample showed that the soil had a particle size distribution and USCS classification which was unlike any of the soils identified in existing boring logs. This likely indicates that the soil migrated from deeper locations within the levee foundation. The laboratory resistivity results also aligned well with the ERT field survey results which suggests that the soils present in the sand boil are the same soils which are present in the disturbed zone shown in the ERT field results. Therefore, ERT may be a valuable non-destructive method to evaluate whether internal erosion or increased seepage is occurring through a levee. Although it was not possible in this case, it is recommended that a future study compare the ERT results before and after a large flood event to determine if damage could be detected based on the differences in the surveys. Ground truthing in the form of additional borings or excavation pits is also recommended in the future to further confirm these results.

ACKNOWLEDGMENTS

REFERENCES

American Association of State Highway and Transportation Officials (AASHTO) (2013). *Standard Method of Test for Determining Minimum Laboratory Soil Resistivity, T-288-12.*

Abdeltawab, S. (2013). "Karst Limestone Geohazards in Egypt and Saudi Arabia." *International Journal of Geoengineering Case Histories*, 2(4), 258-269.

Advanced Geosciences, Inc. (2009). *Instruction Manual for EarthImager 2D Version 2.4.0 Resistivity and IP Inversion Software.*

ASTM International (2011). *Standard Practice for Classification of Soils for Engineering Purposes (Unified Soil Classification System), ASTM D2487-11.*

ASTM International (2017). *Standard Test Method for Particle-Size Distribution (Gradation) of Soils Using Sieve Analysis, ASTM D6913-17.*

ASTM International (2017). *Standard Test Method for Particle-Size Distribution (Gradation) of Fine-Grained Soils Using the Sedimentation (Hydrometer) Analysis, ASTM D7928-17.*

ASTM International (2012). *Standard Test Method for Field Measurement of Soil Resistivity Using the Wenner Four-Electrode Method, ASTM G57-06.*

Blanchette, D. (2016). "Half-mile logjam alters Sangamon River's course." *The State Journal-Register.*

Binley, A., and Kemna, A. (2005). "DC resistivity and induced polarization methods." *Hydrogeophysics*, Springer, Netherlands, 129-156.

Bishop, H., Bruns, E., Kirkeeng, T., Manasco, N., and Theiling, C. (2015). "Lower Sangamon River Regional Sediment Management (RSM) Program.", *15th Biennial Governor's Conference on Management of Illinois River System. U.S. Army Corps of Engineers*, Rock Island District.

Constable, S. C., Parker, R. L., and Constable, C. G. (1987). "Occam's inversion: A practical algorithm for generating smooth models from electromagnetic sounding data." *Geophysics*, 52(3), 289-300.

Edwards, L. (1977). "A modified pseudosection for resistivity and IP." *Geophysics*, 42(5), 1020-1036.

Everett, M. E. (2013). "Electrical Resistivity Method." *Near-Surface Applied Geophysics*, *Chapter 4,* Cambridge University Press, New York, NY, 70-102.

Frankie, W. T., Jacobson, R. J., Killey, M. M., Luman, D.E., Barnhardt, M. L., Lasemi, Z., Norby, R. D., Phillips, M. A., and Crockett, J. E. (1996). "Guide to the Geology of the Beardstown Area, Cass, Schuyler, and Brown Counties, Illinois." *Dept. of Natural Resources*, Illinois State Geological Survey.

Jangea, J. (2003). "Silt slowly burying river town." *The Chicago Tribune*.

Karim, M.Z. and Tucker-Kulesza, S. (2018). "Soil erodibility characterization using electrical resistivity imaging," *J. Geotech. Geoenviron. Eng.*, 144(4).

Kermani, B., Coe, J. T., Nyquist, J. E., Sybrandy, L., Berg, P. H., and McInnes, S. E. (in press). "Evaluation of Unknown Bridge Foundations Using Electrical Resistivity Imaging." *J. Environmental & Engineering Geophysics*.

Kibria, G. and Hossain, M.S. (2016). "Quantification of degree of saturation at shallow depths of earth slopes using resistivity imaging technique." *J. Geotech. Geoenviron. Eng.*, 142(7).

Kibria, G., and Hossain, M. S. (2012). "Investigation of geotechnical parameters affecting electrical resistivity of compacted clays." *J. Geotech. Geoenviron. Eng.*, 138(12), 1090-0241.

Kolb, C. R. (1975). "Geologic control of sand boils along Mississippi River Levees." Army Engineer Waterways Experiment Station, Report AD-A014 274, Vicksburg Mississippi,.

Loke, M.H., Acworth, I., and Dahlin, T. (2003). "A comparison of smooth and blocky inversion methods in 2D inversion of resistivity data," *Exploration Geophysics,* 34(1), 182-187.

Lee, Ming. T. (1982). "Sediment Conditions in the Sanganois Conservation Area, Cass and Mason Counties, Illinois." *SWS Contract Report 290*, State Water Survey Division, Surface Water Section at the University of Illinois, Illinois Department of Energy and Natural Resources,.

Mansur, C. I., Postol, G. and Salley, J. R. (2000). "Performance of Relief Well Systems along Mississippi River Levees." *J. Geotech. Geoenviron. Eng.*, 126(8).

Miller, James A. (1973). "Quaternary History of the Sangamon River Drainage System, Central Illinois" *Illinois State Museum Reports of Investigations*, 27. Springfield, IL.

Mofarraj Kouchaki, B., Bernhardt-Barry, M.L., Wood, C.M., and Moody, T. (2019). "A laboratory investigation of factors influencing the resistivity of different soil types," *Geotechnical Testing Journal,* 42(4).

Richards, K.S., and Reddy, K. R. (2007). "Critical appraisal of piping phenomena in earth dams." *Bulletin of Engineering Geology and the Environment*, 66(4), 381-402.

Rutherford, C., Pinter, N., Gamez, J., Harder, L. F., Lobbestael, A., Musgrove, M., Tinoco, R. O., Bernhardt, M.L., Mofarraj, B., Rosenblad, B. L., Uong, M. D., and Heddlesten, A. (2016). *Preliminary Observations of Levee Performance and Damage following the 2015-16 Midwest Floods in Missouri and Illinois*, GEER Association, USA.

Schaefer, J. A, O'Leary, T. M. and Robbins, B.A. (2017). "Assessing the Implications of Sand Boils for Backward Erosion Piping Risk." *Geo-Risk 2017 GSP 285*, 124-136.

Sirieix, C., Genelle, F., Barral, C., Touze-Foltz, N., Riss, J., and Begassat, B. (2015). Characterizing the ageing of a geosynthetic clay linter through electrical resistivity." *Canadian Geotechnical Journal*, 53(3), 423-430.

Snapp, M., Tucker-Kulesza, S., and Koehn, W. (2017). "Electrical resistivity of mechanically stabilized earth wall backfill." *J. Applied Geophysics*, *141*, 98-106.

Tucker, S., Briaud, J.-L., Hurlebaus, S., Everett, M., Arjwech, R. (2015). "Electrical resistivity and induced polarization imaging for unknown bridge foundations," *J. Geotech. Geoenviron. Eng*, 141(5).

Turnbull, W. J. and Mansur, C. I. (1959). "Investigation of Underseepage – Mississippi River Levees" *Journal of the Soil Mechanics and Foundations Division*, 85(4), 41-94.

United States Army Corps of Engineers (USACE) (2000). *Design and Construction of Levees, Manual No. 1110-2-1913*.

Yeagle, Patrick (2014). "The river Lincoln loved. The state's plan to make the Sangamon a destination." *Illinois Times*, <http://illinoistimes.com>.

INTERNATIONAL JOURNAL OF
GEOENGINEERING
CASE HISTORIES